Oxygen stoichiometry, ferromagnetism, and transport properties of $La_{2-x}NiMnO_{6+\delta}$

R. I. Dass, J.-Q. Yan, and J. B. Goodenough
Texas Materials Institute, ETC 9.102, 1 Texas Longhorns #G3800, University of Texas at Austin, Austin, Texas 78712-1063, USA
(Received 9 April 2003; published 21 August 2003)

Nominal La_2NiMnO_6 prepared by solid-state reaction in air in accordance with earlier reports is shown to contain excess oxygen as well as the coexistence of two ferromagnetic phases of comparable Curie temperatures, one monoclinic and the other rhombohedral. As originally predicted, ordering of Ni^{2+} and Mn^{4+} ions gives ferromagnetic Ni^{2+}-O-Mn^{4+} interactions and transforms the orthorhombic *Pbnm* space group to monoclinic $P2_1/n$ with $\beta \approx 90°$ and the rhombohedral $R\bar{3}c$ space group to $R\bar{3}m$ or $R\bar{3}$. Synthesis by the Pechini method in Ar, air, and O_2 atmospheres under different thermal treatments also consistently gave $O_{6+\delta}$; the lowest $\delta = 0.05(1)$ was attained for a single $P2_1/n$ phase reacted under Ar at 1350 °C. Lowering the mean *A*-site atomic radius in $La_{2-x}\square_xNiMnO_6$ and Nd_2NiMnO_6 also stabilizes the monoclinic phase, and near oxygen stoichiometry was attained in $La_{2-x}\square_xNiMnO_6$ for $x \approx 0.09$. Excess oxygen is accommodated in the perovskite structure by the creation of cation vacancies, and it is shown that lanthanum vacancies create deep three-hole acceptor traps. Comparison with the double perovskite La_2CoMnO_6 and $La_2NiRuO_{6+\delta}$ versus La_2CoRuO_6 signals that stabilization of lanthanum vacancies is associated with a Ni^{3+}/Ni^{2+} redox couple that is stabilized by a counter octahedral-site cation *M* having a strong covalent component to its *M*-O bonding. It is therefore proposed that in the presence of Ni^{2+}, but not Co^{2+}, a lanthanum vacancy is stabilized by the formation of two holes trapped deeply in molecular orbitals of an O_{12} cluster of the oxygen atoms that neighbor a lanthanum vacancy. Transport data also indicate a lowering of the separation of the Mn^{4+}/Mn^{3+} and Ni^{3+}/Ni^{2+} redox couples from $E_g \geqslant 0.8$ eV to $E_g \approx 0.3$ eV in the ordered Ni^{2+}, Mn^{4+} array. This lowering and a motional enthalpy $\Delta H_{mn} \approx 0.1$ eV of electrons is attributed to locally cooperative Jahn-Teller deformations of low-spin Ni^{3+} and high-spin Mn^{3+} octahedral sites. The magnetization M(5 K, 50 kOe) is lowered by both local atomic disorder and the formation of antiphase boundaries. It is shown that a prolonged anneal at 800 °C reduces the local atomic disorder, but it does not remove the antiphase boundaries. Synthetic strategies to increase the magnetization must be designed to reduce the concentration of antiphase boundaries and cation vacancies as well as the atomic disorder.

DOI: 10.1103/PhysRevB.68.064415 PACS number(s): 75.30.Cr, 72.80.Ga, 75.30.Et, 75.30.Kz

I. INTRODUCTION

The two earliest studies of La_2NiMnO_6 were independently motivated by a desire to test the just-postulated rules for the sign of the superexchange interaction by making a ferromagnetic insulator $La_2Ni^{2+}Mn^{4+}O_6$ with ordered Ni^{2+} and Mn^{4+} ions on the octahedral sites of a perovskite. The first study was made on the system $LaNi_xMn_{1-x}O_3$, which showed ferromagnetic order with a magnetization approaching the spin-only value for valences Mn^{3+} and low-spin Ni^{3+} over the entire range $0.2 \leqslant x \leqslant 0.5$. Since there was no evidence of long-range atomic order and both Mn^{4+}-O-Mn^{4+} and Ni^{2+}-O-Ni^{2+} interactions would be antiferromagnetic, it was assumed that La_2NiMnO_6 was orthorhombic and contained disordered low-spin Ni^{3+} and Mn^{3+} ions; both of these octahedral-site ions contain a single electron in a twofold-degenerate *e* orbital, so they would couple ferromagnetically to one another by vibronic superexchange.

In this earliest study,[1,2] the La_2NiMnO_6 samples were prepared by solid-state reaction at 1100 °C in air followed by an anneal at 800 °C. The O-orthorhombic ($a < c/\sqrt{2} < b$ in space group *Pbnm*) was distinguished from the O′-orthorhombic ($c/\sqrt{2} < a < b$) phase found in the orbitally ordered oxygen-stoichiometric parent compound $LaMnO_3$. An impurity La_2NiO_4 phase was observed only after post-annealing in vacuum at 800 °C. An observed magnetization in 11 kOe at 4 K was $4.56\mu_B$/f.u., somewhat smaller than the spin-only value of $5\mu_B$/f.u. for either disordered Ni^{3+} and Mn^{3+} or ordered Ni^{2+} and Mn^{4+}.

The second early study was performed by Blasse[3] who synthesized nearly oxygen-stoichiometric La_2NiMnO_6 by solid-state reaction in air at 1000 °C followed by an anneal at 800 °C for an undisclosed period of time. From paramagnetic susceptibility, he obtained a Curie constant $C = 3.10$ emu mol^{-1} K^{-1} ($\mu_{\text{eff}} = 4.90\mu_B$) and a ferromagnetic Weiss constant $\theta = 310$ K; the highest saturation magnetization he obtained at 4 K was $4.37\mu_B$/f.u. Although the magnetization measurements do not distinguish between disordered low-spin Ni^{3+} and high-spin Mn^{3+} on the one hand and ordered Ni^{2+} and Mn^{4+} on the other, Blasse concluded from the μ_{eff} that he had demonstrated $La_2Ni^{2+}Mn^{4+}O_6$ with a large degree of atomic order; ions in antisite positions would have antiferromagnetically coupled spins.

In fact, recent electrochemical data[4] show that the reaction

$$Ni^{2+} + Mn^{4+} = Ni^{3+} + Mn^{3+} \quad (1)$$

is biased to the left by about 0.8 eV, and several studies with ^{55}Mn NMR,[5,6] extended x-ray absorption fine structure (EXAFS) and x-ray absorption near-edge structure (XANES),[7] and neutron diffraction[8] support Blasse's assignment. However, Sonobe and Asai[6] observed the coexistence

of orthorhombic and rhombohedral phases with the volume fraction of the rhombohedral phase increasing with the partial pressure of oxygen, pO_2, in samples annealed at 900 °C in flowing O_2. Both phases were ferromagnetic. Blasco *et al.*[8] prepared $La_2NiMnO_{6+\delta}$ samples by the Pechini method,[9] which were also annealed in flowing O_2 at 900 °C for 2 days followed by different post-annealing treatments. They found the same two phases, but identified the O-orthorhombic as monoclinic $P2_1/n$ and the rhombohedral as $R\bar{3}m$ or $R\bar{3}$ to allow for two distinguishable octahedral sites. They concluded that both phases contained ordered Ni^{2+} and Mn^{4+}. A $La_2NiMnO_{6.10}$ sample showed a $P2_1/n$ to rhombohedral transition near room temperature and a $T_c = 260$ K. They concluded that both phases contained about 16% atomic disorder in their sample. The better-ordered sample of Asai[5] had a $T_c = 275$ K. Blasco *et al.*[8] also found that post-annealing in N_2 gave the impurity phase La_2NiO_4.

On the other hand, Joseph Joly[10] recently reported a ferromagnetic orthorhombic phase with a well-defined $T_c \approx 150$ K that had been prepared by the glycine-nitrate method at temperatures $T < 500$ °C in air. The paramagnetic susceptibility below 573 K of a sample prepared at 400 °C gave a $\mu_{\text{eff}} = 5.01\mu_B$ and a $\theta = 192$ K. However, annealing at 1300 °C in air resulted in rhombohedral symmetry with a $T_c \approx 280$ K, a $\mu_{\text{eff}} = 5.05\mu_B$, and a $\theta = 313$ K as measured below 723 K. Samples annealed in the range $500\,°\text{C} \leqslant T < 1300\,°\text{C}$ contained both ferromagnetic phases. Unfortunately, the saturation magnetizations of the two phases were not given. The authors speculated that the orthorhombic low-T_c phase contained Mn^{4+} and Ni^{2+} whereas the more stable rhombohedral high-T_c phase contained Mn^{3+} and low-spin Ni^{3+}. If one of the two phases contains Ni^{3+} and Mn^{3+}, it would more probably be the low-T_c phase since a high T_c has been shown to be characteristic of phases with atomically ordered Ni^{2+} and Mn^{4+}.

The present study was undertaken in an attempt to clarify the chemistry of La_2NiMnO_6; our syntheses all gave nominal $La_2NiMnO_{6+\delta}$ compositions suggestive of the dissolution of amorphous La_2O_3 and/or La_2NiO_4. We were able to obtain nearly oxygen-stoichiometric $La_{2-x}\square_xNiMnO_6$ samples with $x \approx 0.09$. These results force us to ask why $La_2CoMnO_{6-\delta}$ is stabilized in air[11] whereas $La_2NiMnO_{6+\delta}$ is found; the Co^{3+}/Co^{2+} couple is less stable than the Ni^{3+}/Ni^{2+} couple. Because low-spin Ni^{3+}: t^6e^1 and high-spin Mn^{3+}: t^3e^1 are both strong Jahn-Teller ions, the possible role of cooperative site deformations is investigated. In addition, we have observed that double perovskites may contain atomically ordered antiphase regions separated by antiphase boundaries across which the neighboring ferromagnetic regions are coupled antiferromagnetically in an external magnetic field $H = 0$.[12,13] The possible influence of antiphase boundaries in nominal La_2NiMnO_6 is also considered.

II. EXPERIMENTAL PROCEDURES AND RESULTS

A. Synthesis

Compounds of the system $La_{2-x}\square_xNiMnO_{6+\delta}$ ($0 \leqslant x \leqslant 1/10$), $La_2Ni_{0.90}Mn_{1.10}O_{6+\delta}$, and $Nd_2NiMnO_{6+\delta}$ were synthesized by the Pechini method[9] with $La(NO_3)_3 \cdot 6.03(1)H_2O$ or precalcined Nd_2O_3 dissolved in dilute nitric acid, $Ni(NO_3)_2 \cdot 5.99(1)H_2O$, and $Mn(CH_3COO)_2 \cdot 3.54(1)H_2O$ as the starting materials; the Nd_2O_3 powders were precalcined in air at 1000 °C for 12 h. The water of crystallization of the salts was determined by thermogravimetric analysis (TGA) with a heating rate of 1 °C/min in flowing air for lanthanum (III) nitrate and in a flowing mixture of 5% H_2/Ar for nickel (II) nitrate and manganese (II) acetate. Stoichiometric quantities of the salts were dissolved in de-ionized water; a little dilute nitric acid was then added to ensure complete dissolution of the acetate. In this synthesis, 1.5 times the stoichiometric amount of citric acid was then added to the stirring emerald-green solution to accomplish complete chelation. Ethylene glycol was added to the emerald-green chelated solution, and this solution was then heated to approximately 150 °C to allow the chelates to undergo polyesterification as well as to remove excess water. The resulting yellowish-green-brown gel was completely dried in an oven, ground, and slowly decomposed in air at 375 °C for 24 h. The products, a brown powder for $x = 0$ and dark-brown powders for $x = 1/12$ and 1/10, $La_2Ni_{0.90}Mn_{1.10}O_{6+\delta}$, and $Nd_2NiMnO_{6+\delta}$, were ground, pressed into half-inch-diameter pellets 2–5 mm thick, and annealed in different flowing atmospheres at the temperatures and for the times indicated in Table I. With the exception of the quenched samples LNM-Q1 and LNM-Q2, all samples were cooled to room temperature in their respective atmospheres at the cooling rates indicated in Table I. Samples synthesized at $T \leqslant 550$ °C were brown while those synthesized at $550\,°\text{C} < T \leqslant 1000\,°\text{C}$ were black; all samples synthesized at $T \leqslant 1000$ °C were soft. However, all samples synthesized at $T > 1000$ °C were gray-black and those synthesized at $T \geqslant 1300$ °C were also dense. Samples of $x = 0$ were also prepared by solid-state reaction; powders of La_2O_3 precalcined in air at 1000 °C for 12 h, Mn_2O_3, and NiO were ground together in stoichiometric ratios. The mixed powders were then pressed into half-inch-diameter pellets 2–3 mm thick and annealed in different flowing atmospheres at the temperatures and for the times also shown in Table I. The resulting pellets were gray-black. The data for only a few samples synthesized by the Pechini method and solid-state reaction are included in Table I.

The oxygen stoichiometry, the $6+\delta$ of Table I, was determined by complete reduction in flowing 5% H_2/Ar to a mixture of La_2O_3 or Nd_2O_3, MnO, and Ni metal in a Perkin-Elmer Series 7 TGA at a heating rate of 1 °C/min to 1000 °C. The oxygen stoichiometry of all samples annealed at $T \geqslant 1100$ °C was reproducible. The δ for samples sintered at $550\,°\text{C} < T \leqslant 800\,°\text{C}$ was difficult to resolve because of the adsorbed water on the large surface area of the powders as well as the incorporation of a small amount of undecomposed carbon from the gel; however, a $\delta \geqslant 0.30$ for these samples was reproducible.

B. Structure

The identification of all room-temperature phases and determination of their lattice parameters were accomplished

TABLE I. The synthesis conditions and room-temperature structural properties of $La_{2-x}\square_xNiMnO_{6+\delta}$, $La_2Ni_{0.90}Mn_{1.10}O_{6+\delta}$, and $Nd_2NiMnO_{6+\delta}$ prepared under different conditions.

Sample	Synthesis conditions	Oxygen content, $6+\delta$	Space group	a (Å)	b (Å)	c (Å)	α (°)	β (°)	V (Å^3)
			$La_{2-x}\square_xNiMnO_{6+\delta}$ $x=0$ Sol gel						
LNM-R1	1350 °C(6 h), Ar, cool 180 °C/h	6.05(1)	$P2_1/n$	5.517(1)	7.748(1)	5.466(1)		90.01(1)	233.65(12)
LNM-R2	1350 °C(6 h), Ar, cool 20 °C/h	6.07(1)	$P2_1/n+R$-3(R-3m)						
LNM-A1	1350 °C(6 h), air, cool 180 °C/h	6.08(1)	$P2_1/n+R$-3(R-3m)						
LNM-A2	1100 °C(48 h), air, cool 20 °C/h	6.19(1)	R-3(R-3m)$+P2_1/n$						
LNM-A3	LNM-A2 at 800 °C(504 h), air, cool 180 °C/h	6.22(1)	R-3(R-3m)$+P2_1/n$						
LNM-A4	LNM-Q2 at 800 °C(168 h), air, cool 180 °C/h	6.10(1)	$P2_1/n$	5.515(1)	7.738(1)	5.462(1)		90.02(1)	233.09(12)
LNM-Q1	1350 °C(12 h), air, quenched in liquid N_2	6.08(1)	$P2_1/n+R$-3(R-3m)						
LNM-Q2	1450 °C(4 h), air, quenched in liquid N_2	6.08(1)	$P2_1/n$	5.517(1)	7.743(1)	5.463(1)		90.03(1)	233.37(12)
LNM-O1	1350 °C(24 h), O_2, cool 20 °C/h	6.09(1)	$P2_1/n+R$-3(R-3m)						
LNM-O2	1350 °C(24 h), O_2, cool 180 °C/h	6.08(1)	$P2_1/n+R$-3(R-3m)						
LNM-LT1	425 °C(110 h), air, cool 180 °C/h		Amorphous						
LNM-LT2	600 °C(144 h), air, cool 180 °C/h	$\geqslant$6.32(5)	R-3(R-3m)	5.451(3)			60.75(2)		116.47(23)
LNM-LT3	725 °C(80 h), air, cool 180 °C/h	$\geqslant$6.30(5)	R-3(R-3m)	5.446(3)			60.84(2)		116.38(23)
			Solid state						
LNM-SA1	1100 °C(48 h), air, cool 20 °C/h	6.10(1)	$P2_1/n+R$-3(R-3m)	Small	$La_2NiO_{4+\delta}$	impurity			
LNM-SA2	LNM-SA1 at 800 °C(252 h), air, cool 180 °C/h	6.09(1)	$P2_1/n+R$-3(R-3m)	Small	$La_2NiO_{4+\delta}$	impurity			
LNM-SA3	1100 °C(96 h), air, cool 20 °C/h	6.08(1)	$P2_1/n+R$-3(R-3m)						
			$x=1/12$						
L2NM-O1	1350 °C(24 h), O_2, cool 20 °C/h	6.03(1)	$P2_1/n$	5.515(1)	7.742(1)	5.463(1)		90.05(1)	233.25(12)
			$x=1/10$						
L1NM-O1	1350 °C(24 h), O_2, cool 20 °C/h	5.97(1)	$P2_1/n$	5.516(1)	7.742(1)	5.464(1)		90.04(1)	233.34(12)
			$La_2Ni_{0.90}Mn_{1.10}O_{6+\delta}$						
LNM55-A1	1100 °C(48 h), air, cool 20 °C/h	6.18(1)	$P2_1/n+R$-3(R-3m)						
			$Nd_2NiMnO_{6+\delta}$						
NNM-O1	1350 °C(12 h), O_2, cool 60 °C/h	6.25(1)	$P2_1/n$	5.410(1)	7.676(1)	5.481(1)		90.03(1)	227.61(12)
NNM-A1	1100 °C(48 h), air, cool, 20 °C/h	6.16(1)	$P2_1/n$	5.413(1)	7.671(1)	5.482(1)		90.05(1)	227.63(12)
NNM-LT1	600 °C (110 h), air, cool 180 °C/h	$\geqslant$6.35(5)	$P2_1/n$	5.410(1)	7.675(1)	5.500(1)		90.10(1)	228.37(12)

with a Philips PW 1729 powder x-ray diffractometer equipped with a pyrolytic graphite monochromator and Cu $K\alpha$ radiation ($\lambda=1.54059$ Å); NaCl was the internal standard. Data were collected in steps of 0.020° over the range $10°\leqslant 2\theta\leqslant 100°$ with a count time of 15 s per step. Peak profiles were fitted with the program JADE and lattice parameters were refined by a least-squares method developed by Novak and Colville.[14] The lattice constants of the different samples are also given in Table I.

No superstructure lines were observed in any of the samples due to the small difference in the mean scattering factors of Ni and Mn.[15] All $x=0$ samples heated to $T\geqslant 800$ °C in flowing O_2 or air were biphasic with the two perovskite phases being easily refined within the rhombohedral $R\bar{3}c$ or $R\bar{3}m$ or $R\bar{3}$ ($Z=1$) space group with an $\alpha\approx 60°$ and O-orthorhombic $Pbnm$ or monoclinic $P2_1/n$ ($Z=2$) with a $\beta\approx 90°$, Fig. 1, in agreement with Blasco *et al.*;[8] samples annealed at 800 °C in air for 3 weeks (504 h) were still biphasic. A random distribution of Ni and Mn over the octahedral sites of the perovskite structure occurs in O-orthorhombic $Pbnm$ and $R\bar{3}c$ while an ordering of Ni^{2+} and Mn^{4+} into distinguishable sites can be accommodated in $P2_1/n$ and $R\bar{3}$ or $R\bar{3}m$. As both phases are ferromagnetic with Ni^{2+} and Mn^{4+} ions, we designate the structures $P2_1/n$ and $R\bar{3}m$ or $R\bar{3}$. A nominal La_2NiMnO_6 sample fired at 1350 °C in Ar, LNM-R1, was single-phase to x-ray diffraction and could be refined within $P2_1/n$ with a $\beta\approx 90°$. All

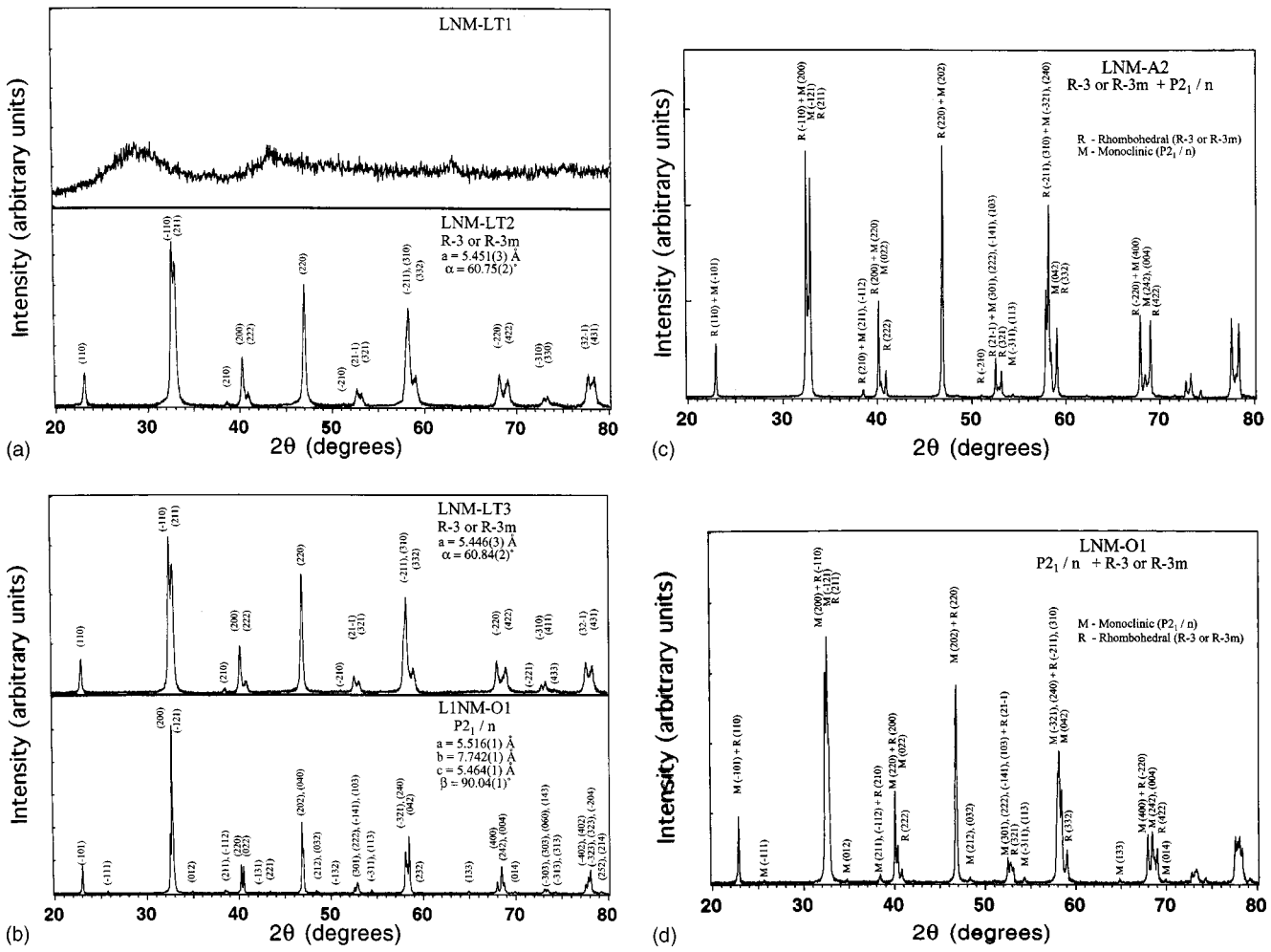

FIG. 1. Room-temperature powder x-ray diffraction patterns of compositions in the system $La_{2-x}\square_xNiMnO_{6+\delta}$ ($0 \leqslant x \leqslant 1/10$).

nominal $La_2NiMnO_{6+\delta}$ samples were oxygen hyperstoichiometric with $\delta \geqslant 0.05(1)$; both δ and the volume fraction of the rhombohedral phase increased with the partial pressure of oxygen, pO_2. Despite firing in Ar, LNM-R1 also had excess oxygen, but with a smaller $\delta = 0.05(1)$. All attempts to prepare a high-temperature, oxygen-stoichiometric phase were unsuccessful. The perovskite structure cannot accept excess oxygen in an interstitial site; therefore, the oxygen nonstoichiometry δ is accommodated by the creation of cation vacancies. Van Roosmalen *et al.*[16,17] have argued that $LaMnO_{3+\delta}$ and $La_{1-x}A_xMnO_{3+\delta}$ (A = alkaline earth) have an equal number of La and Mn vacancies, but other studies by Tofield and Scott[18] and Mitchell *et al.*[19] have reported that the vacancies are preferentially on the La sites and have suggested that the extra extruded La is present as amorphous La_2O_3 that is undetected by a diffraction experiment. If amorphous La_2O_3 is present, then a post-anneal in vacuum or N_2 would give La_2NiO_4 and MnO in addition to a reduced lanthanum-vacancy concentration ($\square_{La}$) in the majority phase; an impurity La_2NiO_4 phase was observed after post-annealing in vacuum in the earliest study[1,2] and after annealing in N_2 by Blasco *et al.*[8]

Therefore, a series of La-deficient samples, $La_{2-x}\square_xNiMnO_{6+\delta}$, was deliberately prepared in flowing O_2 to determine whether a La deficiency would give a well-ordered single phase at high temperature. The La-deficient samples $x = 1/12$ and $1/10$ were single phase and could be refined within the monoclinic space group $P2_1/n$ with a $\beta \approx 90°$, similar to LNM-R1. They were also highly crystalline with narrow x-ray diffraction peaks, e.g., Fig. 1. Sample $x = 1/10$ had a $\delta = -0.03(1)$ while $x = 1/12$ had a $\delta = 0.03(1)$.

Table I shows a nearly constant a parameter and a $\beta \approx 90°$ for all samples of $La_{2-x}\square_xNiMnO_{6+\delta}$ indexed as monoclinic $P2_1/n$. Samples $x = 1/12$ and $1/10$ with La^{3+} vacancies and the highest Ni oxidation states had only a little smaller cell volume than the $P2_1/n$ sample of $x = 0$ prepared in Ar.

All attempts to synthesize a single-phase, high-temperature, rhombohedral $x = 0$ phase were unsuccessful. However, samples of $x = 0$ synthesized in air at $550\,°C < T < 800\,°C$ for more than 80 h, though poorly crystalline, could be refined within the rhombohedral space groups $R\bar{3}$ or $R\bar{3}m$, Fig. 1; they had a $\delta \geqslant 0.30$. This low-temperature rhombohedral phase of $x = 0$ is different from the orthorhombic phase synthesized by Joseph Joly[10] in air at a $T < 500\,°C$. Samples of $x = 0$ synthesized in air at $T \leqslant 550\,°C$

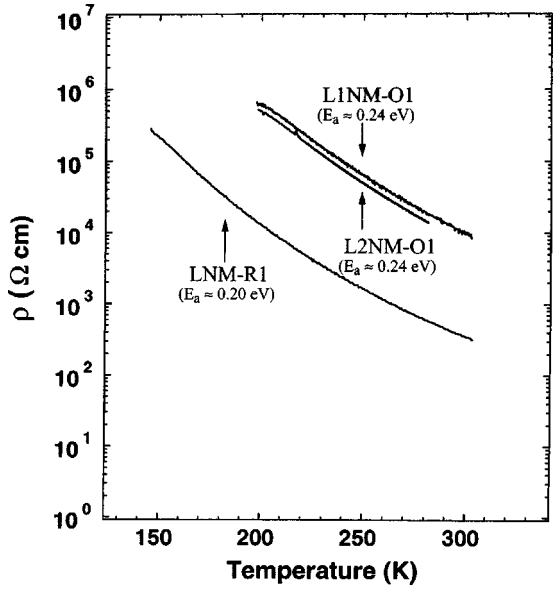

FIG. 2. Variation with temperature of the electrical resistivity $\rho(T)$ for some compositions in the system $La_{2-x}\square_xNiMnO_{6+\delta}$ $(0\leqslant x\leqslant 1/10)$.

in this study were brown in color and amorphous, e.g., LNM-LT1. On annealing in air at 800 °C, these samples became biphasic. A monoclinic $P2_1/n$ phase with $\beta\approx 90°$ prepared in Ar atmosphere contained an excess of oxygen, $\delta\approx 0.05(1)$. However, unquenched samples prepared in air by the Pechini method contained a rhombohedral impurity phase within the monoclinic matrix if the oxygen excess was $0.07\leqslant\delta\leqslant 0.10$ while those prepared with a $\delta>0.10$ contained a monoclinic impurity phase within the rhombohedral matrix. On the other hand, a nearly stoichiometric monoclinic phase can be obtained with 4%–5% La deficiency, which is consistent with earlier observations[18,19] that excess oxygen in the manganese perovskites is accommodated primarily by the introduction of La vacancies with the formation of amorphous La_2O_3. In the case of $La_2NiMnO_{6+\delta}$, the formation of amorphous La_2O_3, which is undetected by a diffraction experiment, may be inferred from the observation of an La_2NiO_4 impurity in vacuum-annealed and N_2-annealed samples prepared at high temperatures in air $[\delta\geqslant 0.07(1)]$. It thus appears that a stable 50:50 $Ni^{2+}+Mn^{4+}$ configuration over the entire sample is difficult to achieve. Although $Nd_2NiMnO_{6+\delta}$ is single phase, the excess oxygen prevents realization of 50:50 $Ni^{2+}+Mn^{4+}$.

C. Transport properties

The resistivity $\rho(T)$ of three single-phase monoclinic samples of $La_{2-x}\square_xNiMnO_{6+\delta}$, Fig. 2, was measured by a four-probe technique with a laboratory-built apparatus in the temperature range $10\text{ K}<T<305\text{ K}$. The samples were first cut into rectangular bars $0.5\times 0.5\times 3.5\text{ mm}^3$ and the four probes were mounted onto the sample surface with tiny In pads. All samples were semiconductors with a high resistance.

For all samples, the Seebeck coefficient $\alpha(T)$, Fig. 3, was obtained with a laboratory-built apparatus as described

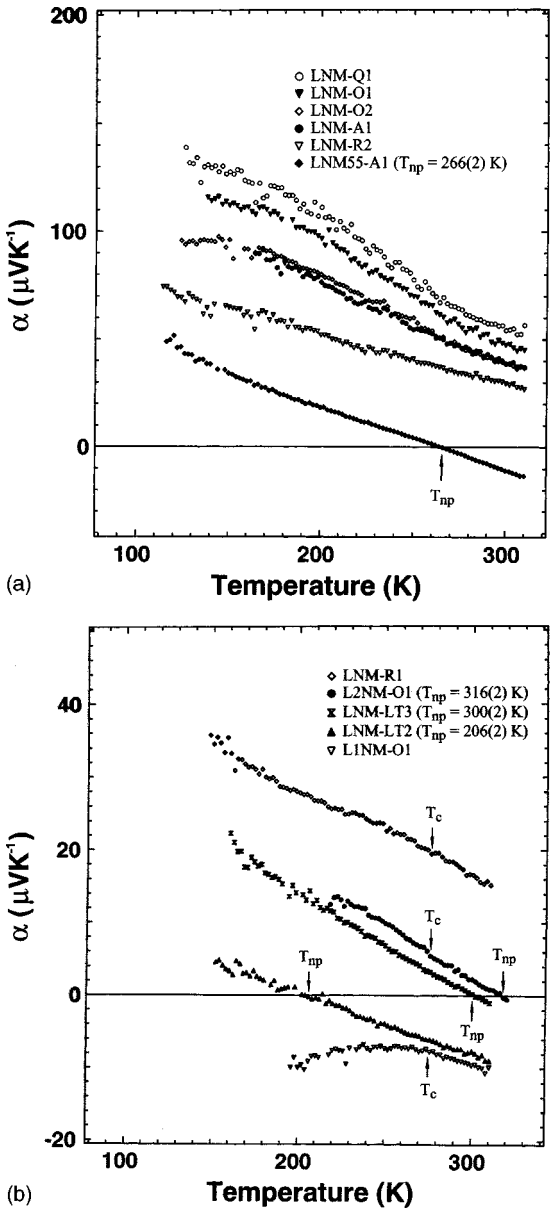

FIG. 3. Variation with temperature of the thermoelectric power $\alpha(T)$ for (a) biphasic and (b) monophasic compositions in the system $La_{2-x}\square_xNiMnO_{6+\delta}$ $(0\leqslant x\leqslant 1/10)$. The ferromagnetic Curie temperature T_c and the *n*-type to *p*-type transition T_{np} are indicated for some of the compositions.

elsewhere.[20] Since all the samples had a high resistance below 305 K, the data became unreliable for most samples below 120 K due to the impedance limits of the apparatus. A correction was applied to compensate for the small contribution to $\alpha(T)$ from the leads.

The $Nd_2NiMnO_{6+\delta}$ and all biphasic samples synthesized by the Pechini method with $x=0$ and $0.07\leqslant\delta\leqslant 0.09$, Fig. 3(a), exhibited a large, positive $\alpha(T)$ that increases on lowering the temperature; the single-phase monoclinic LNM-R1 sample with $\delta=0.05(1)$ also exhibited *p*-type conduction, Fig. 3(b). On the other hand, the low-temperature, rhombohedral phases LNM-LT2 and LNM-LT3 with $\delta\geqslant 0.30$ and $La_2Ni_{0.90}Mn_{1.10}O_{6.18(1)}$ exhibited a transition from negative

to positive thermoelectric power on cooling through $T_{np} \approx 206(2)$ K, 300(2) K, and 266(2) K, respectively. The L1NM-O1, $x = 1/10$ phase, with $\delta = -0.03(1)$, exhibited *n*-type conduction while a $T_{np} \approx 316(2)$ K was observed for L2NM-O1, $x = 1/12$, which had a $\delta = 0.03(1)$.

D. Magnetic data

Magnetic data were taken with a Quantum Design dc superconducting quantum interference device (SQUID) magnetometer in the temperature range $5\ \text{K} \leqslant T \leqslant 700$ K and in applied magnetic fields from -50 kOe to 50 kOe. The *M-H* curves taken at 5 K, Fig. 4, exhibit a low-remanence M_r and coercivity $H_{ci} \leqslant 320$ Oe for all high-temperature phases. Saturation of the magnetization was never attained in any of the samples prepared by the Pechini method, and $M(5\ \text{K}, 50\ \text{kOe}) \leqslant 4.05 \mu_B$/f.u., smaller than the theoretical spin-only value of $5 \mu_B$/f.u., was always observed. This observation contrasts with the earlier studies[1–3] on samples prepared by solid-state synthesis that found $M(5\ \text{K}, 11\ \text{kOe}) = 4.56$ and $4.37 \mu_B$/f.u. Therefore, we also prepared a sample LNM-SA1 by solid-state synthesis under similar conditions and obtained $M(5\ \text{K}, 50\ \text{kOe}) = 4.31 \mu_B$/f.u. Figure 5 shows the *M-H* hysteresis loops for nominal $La_2Ni_{0.90}Mn_{1.10}O_{6+\delta}$ and $Nd_2NiMnO_{6+\delta}$. These samples had $\delta \geqslant 0.16$. Biphasic $La_2Ni_{0.90}Mn_{1.10}O_{6+\delta}$ had a saturation magnetization $M(5\ \text{K}, 50\ \text{kOe}) = 4.17 \mu_B$/f.u.; the $Nd_2NiMnO_{6+\delta}$ samples were single-phase $P2_1/n$, and the *M-H* curves reflect the contribution from the Nd^{3+} ions at 5 K. The magnetic properties of the samples at 5 K are summarized in Table II.

Figure 6 shows the molar magnetization $M(T)$ for the samples of $La_{2-x}\square_x NiMnO_{6+\delta}$ in magnetic fields of 20 Oe and 2500 Oe after cooling in zero field (ZFC) or cooling in the measuring field (FC). Before any measurements were made, the samples were heated to $T = 320$ K to remove any previous magnetic history. The magnetic transition temperatures T_c or T_f of Table II were taken from the inflection point of the low-field ($H = 20$ Oe) data. Long-range ferromagnetic order with $T_c \approx 276(2)$ K and an enhancement of $M(T, 2500\ \text{Oe})$ below 80 K were observed in the three unquenched monoclinic phases. The biphasic LNM-O1 sample of Fig. 6(a) had a smaller enhancement of $M(T)$ below 80 K than that found in sample LNM-R1 with a single monoclinic phase and a lower $M(5\ \text{K}, 50\ \text{kOe})$. The two rhombohedral phases LNM-LT2 and LNM-LT3 had a similar Curie temperature, $272(2)\ \text{K} \leqslant T_c \leqslant 280(2)$ K, but a lower $M(5\ \text{K}, 50\ \text{kOe})$ and a larger enhancement of $M(T)$ below 110 K, Fig. 6(b). The amorphous LNM-LT1 phase exhibited no long-range magnetic order down to 5 K; it remained a Curie-Weiss paramagnet.

The quenched sample LNM-Q2 of Fig. 6(c) shows frustrated magnetic order setting in below $T_{f1} \approx 278(2)$ K with a significant increase in $M(T)$ occurring below 40 K in $H = 2500$ Oe; the ferromagnetic component above 80 K in $H = 2500$ Oe was only increased slightly by an anneal at 800 °C for 168 h, sample LNM-A4. Figure 6(d) shows that the biphasic sample LNM-A2 prepared in air at 1100 °C has a low-field magnetization that decreased slightly after a prolonged anneal at 800 °C in air that increases δ. The sample LNM-SA1 of Fig. 6(e), which was prepared by solid-state synthesis as previously reported, viz., sintered at 1100 °C for 48 h and cooled at 20 °C/h, had the highest $M(5\ \text{K}, 50\ \text{kOe}) = 4.31 \mu_B$/f.u., approaching the values previously reported, but it was triphasic, containing some La_2NiO_4 impurity. Doubling the sintering time to 96 h at

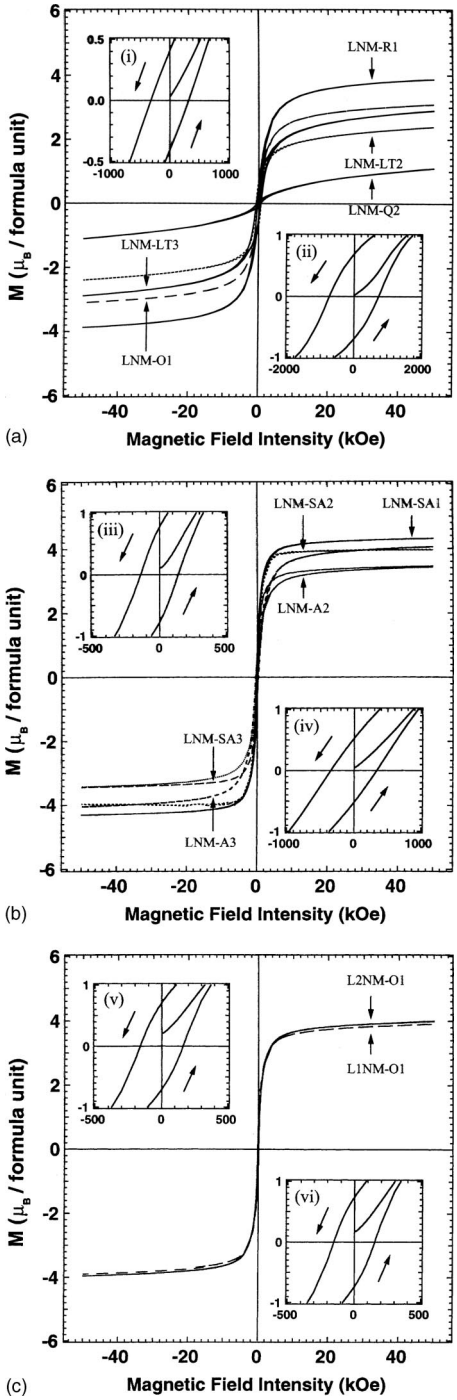

FIG. 4. *M-H* hysteresis loops of some compositions of the system $La_{2-x}\square_x NiMnO_{6+\delta}$ at $T = 5$ K. Insets (i)–(vi) in (a)–(c) show the low coercivities and remanences for (i) LNM-R1, (ii) LNM-LT2, (iii) LNM-SA1, (iv) LNM-A3, (v) L2NM-O1, and (vi) L1NM-O1, respectively.

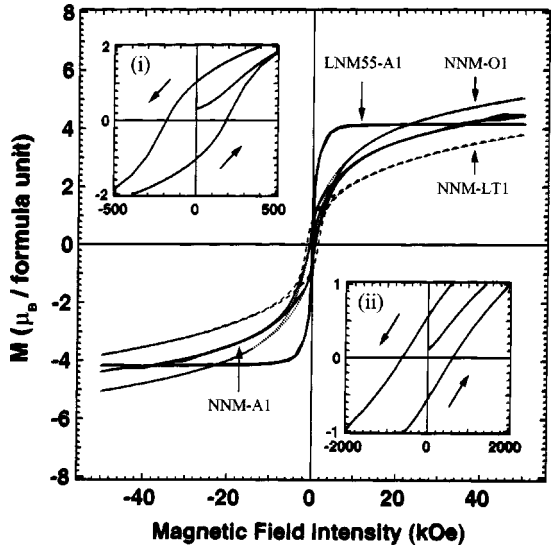

FIG. 5. *M-H* hysteresis loops of some compositions in the systems $La_2Ni_{0.90}Mn_{1.10}O_{6+\delta}$ and $Nd_2NiMnO_{6+\delta}$ at $T=5$ K. Insets (i) and (ii) show the low coercivities and remanences for LNM55-A1 and NNM-O1, respectively.

1100 °C, sample LNM-SA3, removed the La_2NiO_4 impurity without increasing δ, but $M(5\text{ K}, 50\text{ kOe})$ was decreased significantly to $3.45\mu_B$/f.u. The two La-deficient samples L1NM-O1 and L2NM-O1 were single-phase $P2_1/n$ and nearly oxygen stoichiometric, but $M(5\text{ K}, 50\text{ kOe}) \leqslant 4.00\mu_B$/f.u. remained relatively low, and Fig. 6(f) shows an anomalous increase in $M(T)$ below 60 K in $H=2500$ Oe.

Figure 7 shows the $M(T)$ curves in $H=20$ Oe for the $La_2Ni_{0.90}Mn_{1.10}O_{6+\delta}$ sample LNM55-A1 and the nominal $Nd_2NiMnO_{6+\delta}$ samples. The LNM55-A1 sample exhibits a normal ferromagnetic $M(T)$ behavior in $H=20$ Oe and $M(5\text{ K}, 50\text{ kOe})=4.17\mu_B$/f.u. is relatively high, but lower than the value obtained for the nominal $La_2NiMnO_{6+\delta}$ sample, LNM-SA1, prepared by solid-state reaction that contains La_2NiO_4 as an impurity. On the other hand, the $Nd_2NiMnO_{6+\delta}$ phases NNM-O1 and NNM-Al with $\delta=0.25(1)$ and 0.16(1), respectively, both show a marked increase in $M(T)$ on cooling below 80 K in $H=20$ Oe.

III. DISCUSSION AND CONCLUSIONS

In the $Ln_{2-x}\square_xNiMnO_{6+\delta}$ (Ln=lanthanide) double perovskites, the reaction $Ni^{3+}+Mn^{3+}=Ni^{2+}+Mn^{4+}$ is biased strongly enough to the right. These double perovskites are ferromagnetic insofar as Ni^{2+} and Mn^{4+} ions order to give, in accordance with the Goodenough-Kanamori rules, the ferromagnetic $(180°-\phi)$ Ni^{2+}-O-Mn^{4+} superexchange/semicovalent spin-spin interactions.

Samples quenched from $T>1400$ °C have a disordered array of Ni^{2+} and Mn^{4+} ions; they exhibit a frustrated magnetic order below a T_{f1} because the Ni^{2+}-O-Ni^{2+} and Mn^{4+}-O-Mn^{4+} interactions are antiferromagnetic. A prolonged anneal at 800 °C of a quenched sample does not create a long-range ordering of the Ni^{2+} and Mn^{4+} ions. However, in samples with a large degree of long-range order, a prolonged anneal at 800 °C orders isolated Ni^{2+},Mn^{4+} pairs in the bulk, but it does not eliminate antiphase boundaries. The antiphase boundaries couple adjoining ferromagnetic blocks antiferromagnetically in zero applied field to give a small remanence, but a modest applied magnetic field is able to align the blocks leaving 360° spin rotations across an antiphase boundary.[12,13]

Ordering of the Ni^{2+} and Mn^{4+} ions transforms an O-orthorhombic *Pbnm* to monoclinic $P2_1/n$ with a $\beta\approx 90°$ and a rhombohedral $R\bar{3}c$ to $R\bar{3}m$ or $R\bar{3}$. Both the monoclinic and rhombohedral ordered phases are ferromagnetic with comparable values of T_c, i.e., $270\leqslant T_c\leqslant 280$ K. The rhombohedral phase is normally associated with a larger tolerance factor $t\equiv(A\text{-O})/\sqrt{2}(M\text{-O})$, where $(A\text{-O})$ and $(M\text{-O})$ are the mean equilibrium *A*-site and *M*-site bond lengths in the AMO_3 perovskite. Substitution of a smaller Nd^{3+} for La^{3+} reduces t and stabilizes the monoclinic $P2_1/n$ phase. Similarly, the introduction of lanthanum vacancies in $La_{2-x}\square_xNiMnO_{6+\delta}$ reduces $\langle A-O\rangle$, and therefore the tolerance factor, to stabilize the monoclinic $P2_1/n$ phase.

All attempts to prepare oxygen-stoichiometric $Ln_2NiMnO_{6+\delta}$ samples in air or Ar with Ln=La or Nd gave excess oxygen. As it is not possible to introduce oxygen interstitials into the perovskite structure, the excess oxygen can only be accommodated by the introduction of cation vacancies. The fact that prolonged annealing of $La_2NiMnO_{6+\delta}$ may yield La_2NiO_4 as an impurity phase signals that La may be extruded from the lattice as amorphous La_2O_3, leaving a predominance of lanthanum vacancies in the perovskite phase. If the δ extra oxygen atoms per formula unit introduce a predominance of lanthanum vacancies over Ni and Mn vacancies, then the $P2_1/n$ phase would be stabilized relative to the rhombohedral phase. Therefore, the observation of monoclinic and rhombohedral phases in nominal $La_2NiMnO_{6+\delta}$ appears to signal an inhomogeneous preferential extrusion of the lanthanide as La_2O_3. Sample LNM-R1 prepared at 1350 °C in Ar is single-phase $P2_1/n$ with $\delta\approx 0.05(1)$; lanthanum vacancies are assumed to be uniformly distributed throughout this sample with few cation vacancies on the octahedral sites. A similar deduction applies to sample LNM-Q2, which was quenched from 1450 °C. The observation of a single rhombohedral phase in the poorly crystalline samples synthesized at temperatures $T<800$ °C and having $\delta>0.30$ would seem to signal a large concentration of vacancies on both cation sites.

A small reduction of the Ni content in $La_2Ni_{0.90}Mn_{1.10}O_{6.18(1)}$, sample LNM55-A1, prepared in air at 1100 °C did not suppress the incorporation of excess oxygen; this composition was also biphasic, which is suggestive of inhomogeneous extrusion of lanthanum. This sample has $M(5\text{ K}, 50\text{ kOe})=4.17\mu_B$/f.u., which is significantly higher than the $3.42\mu_B$/f.u. of the $La_2NiMnO_{6.19(1)}$ sample LNM-A2 that was prepared with an identical thermal treatment. Although an excess Mn^{4+} on a Ni^{2+} position would produce $3\mu_B$ aligned antiparallel to the magnetization whereas a disordered $Ni^{2+}+Mn^{4+}$ pair in the bulk could give $5\mu_B$ antiparallel to the magnetization, nevertheless the

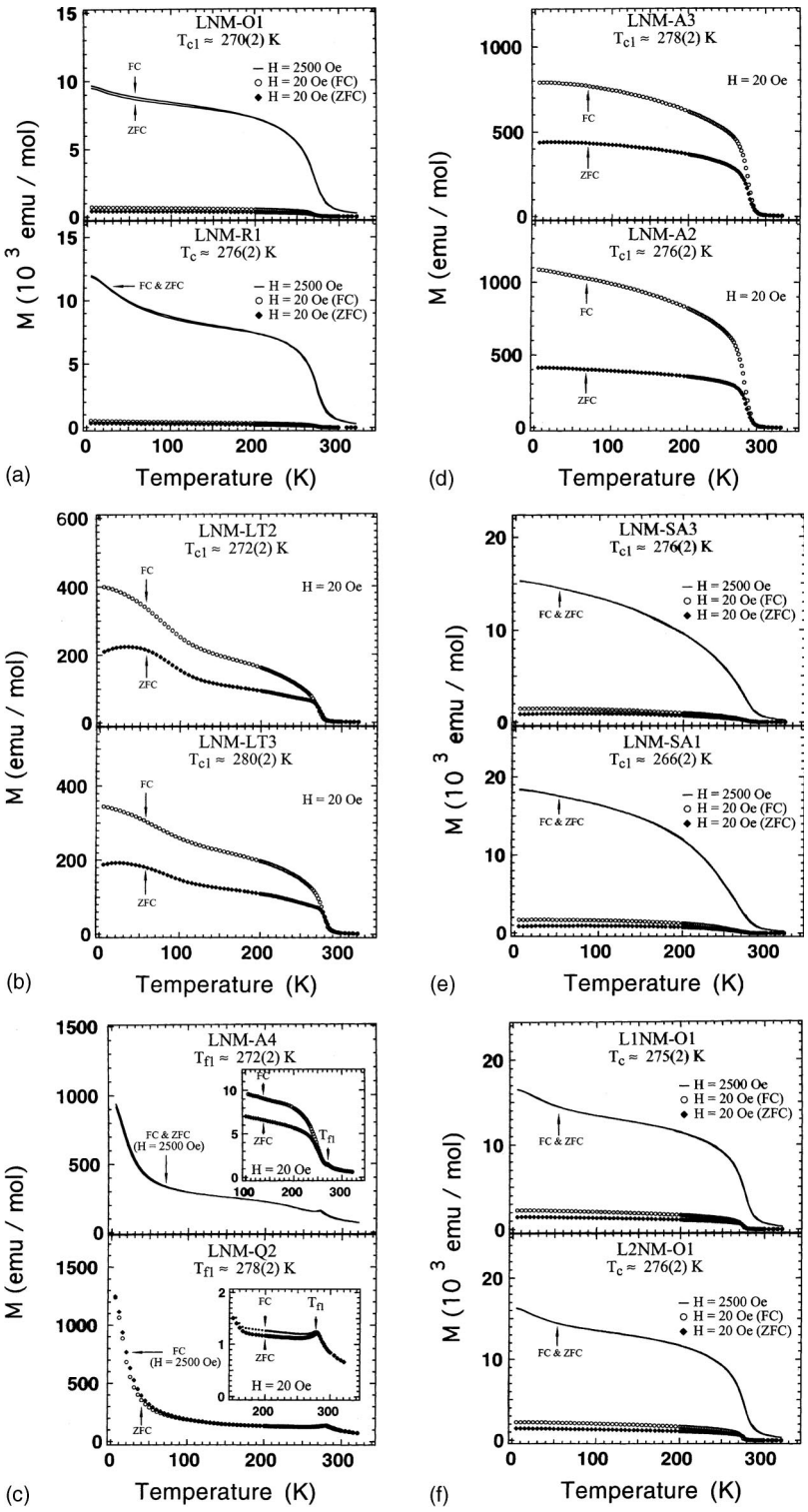

FIG. 6. Temperature dependence of the molar magnetization M under different applied magnetic fields for some compositions in the system $La_{2-x}\square_x NiMnO_{6+\delta}$ $(0 \leqslant x \leqslant 1/10)$.

significantly lower $M(5\,\mathrm{K}, 50\,\mathrm{kOe})$ of LNM-A2 demonstrates a larger degree of disorder for the sample with a ratio Ni/Mn=1. In fact, a prolonged anneal at 800 °C (LNM-A3) elevated $M(5\,\mathrm{K}, 50\,\mathrm{kOe})$ to $4.05\mu_B$/f.u. Antiphase boundaries are immobile at 800 °C. Therefore, this result shows that LNM-A2 contained a large concentration of disordered Ni^{2+}, Mn^{4+} pairs.

The observation of excess oxygen in $LaMnO_{3+\delta}$ can be attributed to a disproportionation reaction 2Mn(III)=Mn(II) + Mn(IV) in the orbitally disordered high-temperature phase, which leads to the oxidation of the Mn(II) to Mn(III). In nominal $La_2NiMnO_{6+\delta}$, all the manganese are Mn(IV), so this mechanism is not available. Moreover, La_2CoMnO_6 is oxygen deficient unless prepared in oxygen atmosphere.[11] In addition, we[21] have performed preliminary experiments with Ru replacing Mn, and here also preparation in air yields $La_2NiRuO_{6.10(1)}$ but $La_2CoRuO_{6.00(1)}$. Therefore, the introduction of lanthanum vacancies $\square_{La}$ must be stabilized more

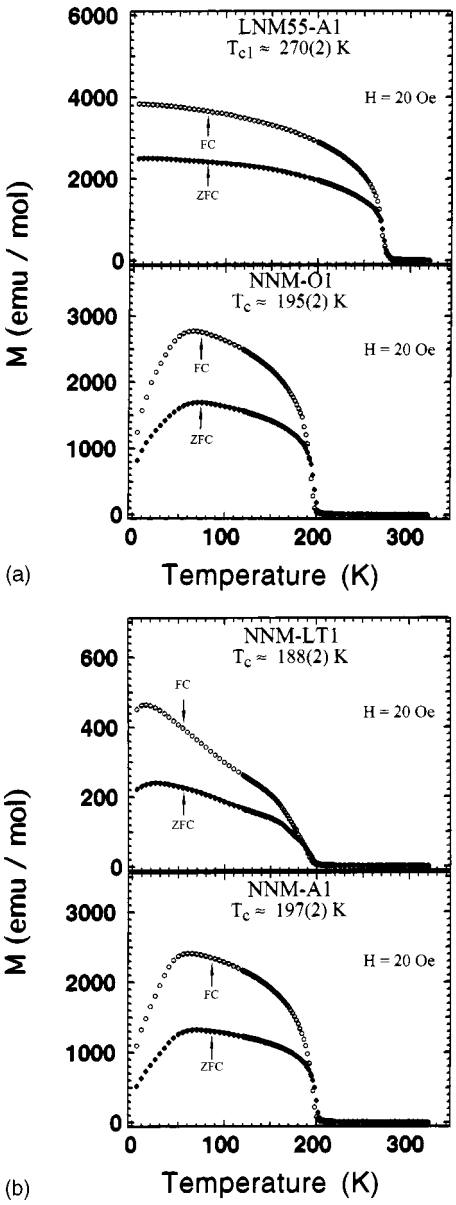

FIG. 7. Temperature dependence of the molar magnetization M under different applied magnetic fields for some compositions in the systems $La_2Ni_{0.90}Mn_{1.10}O_{6+\delta}$ and $Nd_2NiMnO_{6+\delta}$.

strongly by some mechanism associated with the Ni^{3+}/Ni^{2+} couple, which is more stable than the Co^{3+}/Co^{2+} couple. In order to understand how $\square_{La}$ might be more stable in the presence of Ni^{2+} than Co^{2+}, we turn to the transport data.

All the samples were semiconductive. In the single-phase monoclinic samples of $La_{2-x}\square_xNiMnO_{6+\delta}$, cation vacancies act as electron acceptor sites and oxygen vacancies as electron donors. Therefore, it is remarkable that the two nearly oxygen-stoichiometric samples into which 4% and 5% La vacancies have been deliberately introduced have the highest resistivity with, respectively, only *n*-type conduction for $\delta=-0.03(1)$ and *n*-type conduction above $T_{np} \approx 316(2)$ K for $\delta=0.03(1)$. From these data, we draw two conclusions: (1) the La vacancies act as deep traps for the three Ni^{3+} ions each introduces and (2) intrinsic conduction dominates above 200 K with an electron mobility larger than the hole mobility ($\mu_n \gg \mu_p$). On the other hand, the single-phase sample LNM-R1 prepared in Ar atmosphere had a $\delta \approx 0.05(1)$ and remained *p* type to well above room temperature, so we draw an additional conclusion: (3) excess oxygen ($\delta>0$) creates not only La vacancies, but also Mn and/or Ni vacancies that do not trap the Ni^{3+} ions they introduce as strongly as the La vacancies.

The intrinsic polaronic conductivity is $\sigma=\sigma_n+\sigma_p$ with

$$\sigma_n=(A_n/T)\exp(-E_{an}/kT), \quad E_{an}=(1/2)E_g+\Delta H_{mn} \tag{2a}$$

$$\sigma_p=(A_p/T)\exp(-E_{ap}/kT), \quad E_{ap}=(1/2)E_g+\Delta H_{mp} \tag{2b}$$

where E_g is the energy required to transfer an electron from a Ni^{2+} to a Mn^{4+} and the ΔH_m are the motional enthalpies of polaronic charge carriers. At low temperatures, $\sigma \rightarrow \sigma_{ext}$, where the extrinsic conductivity σ_{ext} is dominated by the major dopant supplying charge carriers. The thermoelectric power

$$\alpha=(\alpha_n\sigma_n+\alpha_p\sigma_p)/\sigma \tag{3}$$

has the sign of the dominant charge carrier. A $\mu_n \gg \mu_p$ implies a $\Delta H_{mp}>\Delta H_{mn}$, and an intrinsic resistivity described by $\rho=BT\exp(E_a/kT)$ would have

$$E_a=(1/2)E_g+\Delta H_{mn}. \tag{4}$$

The two La-deficient samples L1NM-O1 and L2NM-O1 have $E_a \approx 0.24$ eV, and an effective $\Delta H_m \approx 0.1$ eV corresponds to an

$$E_g \approx 0.3 \text{ eV} \tag{5}$$

which is a significant reduction from the $\Delta \approx 0.85$ eV splitting between the Mn^{4+}/Mn^{3+} and Ni^{3+}/Ni^{2+} redox couples in oxides as obtained from electrochemical measurements.[22] At lower temperatures, the extrinsic conduction dominates α, revealing the character of the major dopant supplying charge carriers. If a La vacancy traps deeply the three Ni^{3+} ions it introduces, only Mn and/or Ni vacancies supply extrinsic *p*-type carriers and oxygen vacancies *n*-type carriers. Since L1NM-O1 retains $\alpha<0$ to lowest temperatures, it follows that the concentration of oxygen vacancies, $\delta \approx -0.03(1)$/f.u., is greater than that of any Ni^{2+} and/or Mn^{4+} vacancies. Since there are no oxygen vacancies in the L2NM-O1 sample with $\delta \approx 0.03(1)$, the thermoelectric power is $\alpha>0$ below a T_{np} as a result of Ni and/or Mn vacancies.

In a simple cubic array of ordered Ni^{2+} and Mn^{4+} ions, a Mn vacancy would create four Ni^{3+} ions trapped at near-neighbor nickel sites whereas a Ni vacancy would create two Ni^{3+} ions at next-near-neighbor nickel sites. In LNM-R1 with $\delta \approx 0.05(1)$, the larger concentration of excess oxygen

TABLE II. The magnetic properties of $La_{2-x}\square_xNiMnO_{6+\delta}$, $La_2Ni_{0.90}Mn_{1.10}O_{6+\delta}$, and $Nd_2NiMnO_{6+\delta}$ prepared under different conditions. CWP, F, and SG refer to Curie-Weiss paramagnetism, ferromagnetism, and spin glass, respectively. T_{ci}, T_{fi}, $M(50\ \text{kOe})$, M_r, and H_{ci} are the Curie temperature of long-range ferromagnetic order, the spin-glass freezing temperature, the magnetization at 50 kOe, the remanent magnetization, and the coercivity, respectively.

Sample	Type of magnetic behavior	Magnetic transition temperature (K)	M(5 K,50 kOe) (μ_B/f.u.)	M_r (5 K) (μ_B/f.u.)	H_{ci} (5 K) (Oe)	μ_{eff} (μ_B)	θ (K)
			$La_{2-x}\square_xNiMnO_{6+\delta}$				
			$x=0$				
			Sol gel				
LNM-R1	F	$T_c=276(2)$	3.88(2)	0.40(2)	320(5)	5.16(2)	302(2)
LNM-O1	F	$T_{c1}=270(2)$	3.10(2)	0.39(2)	300(5)	5.03(2)	302(2)
LNM-A2	F	$T_{c1}=276(2)$	3.42(2)	0.60(2)	330(5)		
LNM-A3	F	$T_{c1}=278(2)$	4.05(2)	0.52(2)	340(5)		
LNM-A4	SG	$T_{f1}=272(2)$	1.04(1)	0.027	260(5)		
LNM-Q1	F	$T_{c1}=270(2)$	3.10(2)	0.24(2)	290(5)		
LNM-Q2	SG	$T_{f1}=278(2)$	1.10(1)	0.061	460(5)		
LNM-LT1	CWP		0.52(1)	0.002	120(5)		
LNM-LT2	F	$T_{c1}=272(2)$	2.39(2)	0.70(2)	770(5)		
LNM-LT3	F	$T_{c1}=280(2)$	2.90(2)	0.51(2)	690(5)		
			Solid state				
LNM-SA1	F	$T_{c1}=266(2)$	4.31(2)	0.77(2)	140(5)		
LNM-SA2	F	$T_{c1}=268(2)$	3.96(2)	0.52(2)	140(5)		
LNM-SA3	F	$T_{c1}=276(2)$	3.45(2)	0.72(2)	170(5)		
			$x=1/12$				
L2NM-O1	F	$T_c=276(2)$	4.00(2)	0.70(2)	160(5)		
			$x=1/10$				
L1NM-O1	F	$T_c=275(2)$	3.91(2)	0.74(2)	150(5)		
			$La_2Ni_{0.90}Mn_{1.10}O_{6+\delta}$				
LNM55-A1	F	$T_{c1}=270(2)$	4.17(2)	1.04(2)	190(5)		
			$Nd_2NiMnO_{6+\delta}$				
NNM-O1	F	$T_c=195(2)$	5.06(2)	0.56(2)	640(5)		
NNM-A1	F	$T_c=197(2)$	4.48(2)	0.66(2)	720(5)		
NNM-LT1	F	$T_c=188(2)$	3.82(2)	0.86(2)	1390(10)		

appears to create some Ni and/or Mn vacancies in addition to La vacancies, so the temperature range with $\alpha>0$ is larger than that of L2NM-O1, $La_{23/12}\square_{1/12}NiMnO_{6.03(1)}$.

This analysis leaves us with the following four questions: (1) Why is $\mu_n>\mu_p$? (2) Why is the intrinsic gap E_g of L1NM-O1 and L2NM-01 only 0.3 eV compared to 0.85 eV obtained in spinels from electrochemical measurements? (3) Why is the third acceptor level at a La vacancy so deep? (4) Why does $La_2NiMnO_{6+\delta}$ become oxidized whereas $La_2CoMnO_{6-\delta}$ is reduced?

The charge carriers occupy twofold-degenerate e orbitals whether they are holes on low-spin Ni^{3+}:t^6e^1 or electrons on high-spin Mn^{3+}:t^3e^1. Electron jumps between like atoms on next-near-neighbor octahedral sites within an atomically ordered matrix can only occur by transfer across an unlike nearest neighbor. As is illustrated in Fig. 8, these transfers cost less energy where they are enabled by orbital fluctuations at Jahn-Teller ions that are coordinated by breathing-mode shortening and stretching of the (M-O) bond lengths at the unlike central cation. For example, p-type conduction proceeds by transfer of an e electron from Ni^{2+}:t^6e^2 to a Mn^{4+}:t^3e^0 as the oxygen atoms bridging the Mn to its two Ni neighbors move away from the Mn toward the two Ni atoms, step 2 of Fig. 8(a). As the oxygen atoms move back toward the Mn atom, the electron is transferred from the Mn^{3+} ion to a neighboring Ni^{3+} ion, step 3. Similarly, n-type conduction proceeds by an orientation of an occupied e orbital at a Mn^{3+} ion toward a Ni^{2+} ion, which pushes the bridging oxygen toward the Ni^{2+} to lower the energy of its axially oriented e orbital so as to induce transfer of its electron from the Ni^{2+} ion to the Mn^{4+} ion on the opposite side, step 2 of Fig. 8(b). Transfer of the e electron at a Mn^{3+} ion to the Ni^{3+} occurs as the oxygen atoms move back to the equilibrium position for a Ni^{2+} ion, step 3 of Fig. 8(b). A $\mu_n>\mu_p$ means that the motional enthalpy ΔH_m for transfer of an electron from Ni^{2+} to Mn^{4+}, step 2 of Figs. 8(a) and 8(b), is reduced by a Mn^{3+} ion on the opposite side orienting its e orbital along the reaction axis as illustrated in step 2 of

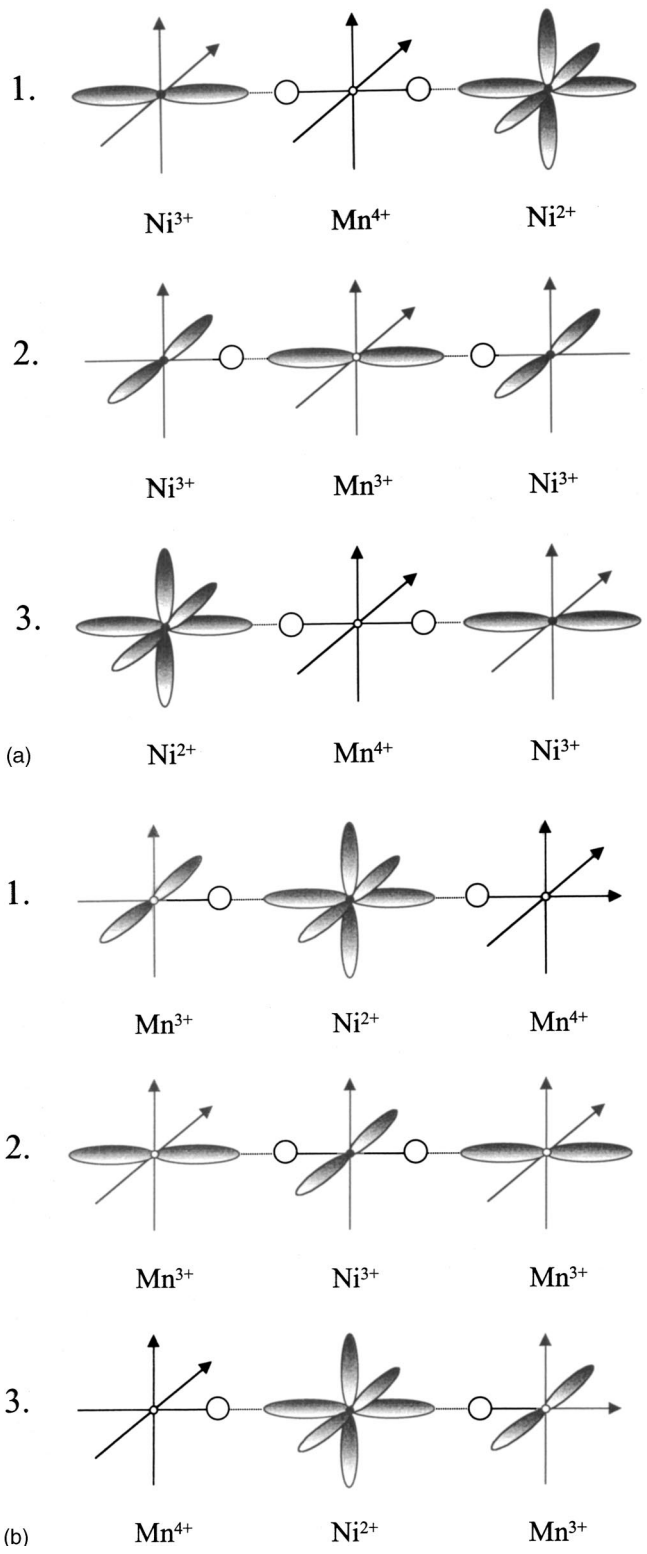

FIG. 8. Coordinated Jahn-Teller distortions that lower the motional enthalpy ΔH_m for (a) hole transfer across a Mn^{4+} ion and (b) electron transfer across a Ni^{2+} ion.

Fig. 8(b). This orientation shortens the Ni-O bond length, which favors transfer of an electron from the Ni^{2+} ion to the Mn^{4+} ion on the opposite side. Reduction of the intrinsic gap from 0.85 eV to $E_g \approx 0.3$ eV also follows from Fig. 8. It is

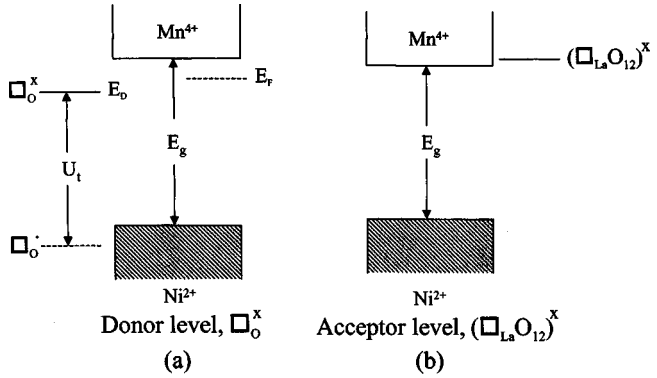

FIG. 9. Schematic energies for the polaronic Mn^{4+}/Mn^{3+} and Ni^{3+}/Ni^{2+} redox couples in the presence of (a) oxygen-vacancy donor and (b) lanthanum-vacancy acceptor clusters.

the locally cooperative Jahn-Teller distortions that aid the transfer of an electron from a Ni^{2+} to a Mn^{4+} near neighbor; the energy of this process is further reduced to 0.1 eV in a mixed-valent system where there is an additional electron involved in the electron-transfer process.

The observation that sample L1NM-O1 remains *n* type clearly signals that the donor $\square_O^x$ level of an oxygen vacancy lies below the acceptor level at a $(\square_{La}O_{12})^x$ cluster, which is an unusual situation. An oxygen vacancy is a two-electron trap, and the electrons occupy Mn sites as Mn^{3+} ions, which are stable in fivefold oxygen coordination.[23] If the oxygen vacancy lies between a Ni and a Mn atom, one electron is deeply trapped at the neighboring Mn atom and the second electron is more loosely bound at a next-near-neighbor Mn^{3+} ion. If the vacancy lies between two Mn atoms, the Mn^{3+} ions on the two Mn sites would be oriented toward the vacancy where they would form a conventional two-electron trap at the vacancy. In either case, there will be a shallow donor level for the two-electron trap $\square_O^x$ separated by an energy U_t from a deeper one-electron trap $\square_O^{\cdot}$, Fig. 9(a).

The character of the acceptor level associated with a lanthanum vacancy $\square_{La}$ is not so obvious. It is useful to begin with the final question, why do we have $La_2NiMnO_{6+\delta}$ and $La_2CoMnO_{6-\delta}$ after firing in air given a Ni^{3+}/Ni^{2+} level lower than a Co^{3+}/Co^{2+} level? To address this question, we note that NiO has been classified as having a charge-transfer gap whereas CoO as having a *U* gap.[24] This classification means that the Ni^{3+}/Ni^{2+} redox energy lies below the $O^{2-}:2p^6$ energy in a point-charge model whereas the Co^{3+}/Co^{2+} level lies above it. As a result, the Ni^{3+}/Ni^{2+} redox energy becomes pinned as a band of antibonding states at the top of the $O^{2-}:2p^6$ bands with strong $Ni:3d$-$O:2p$ hybridization; it is this hybridization that gives the Ni^{3+} ion a low-spin configuration and makes $LaNiO_3$ metallic.[25] A $\square_{La}$ would trap three holes to establish a $(\square_{La}O_{12})^x$ cluster having local charge neutrality. In the presence of a $\square_{La}$, lowering of the local Madelung energy transfers the holes to $O:2p_\pi$ orbitals where they form molecular-orbital O_{12}-cluster states that are antibonding with respect to the O-O interactions. Relatively strong O-O interactions would raise the empty O_{12}-cluster states high enough to create a deep acceptor state with an odd number of holes in the O_{12}

cluster; the trap should have an oxygen spin $S=1/2$. This localized spin would remain paramagnetic, but at lowest temperatures it would contribute in an applied field $H=2500$ Oe to the upturn in $M(T)$ that is observed in all the single-phase $P2_1/n$ samples, each of which has lanthanum vacancies. In La_2CoMnO_6, the low-spin Co(III) ion, on the other hand, has no e electrons, and hybridization with the $O{:}2p_\sigma$ orbitals apparently lifts the empty states to too high an energy for electron transfer to them from the $O{:}2p_\pi$ orbitals. Given this picture, it is proposed here that the stability of an oxidized $La_2NiMnO_{6+\delta}$ and $La_2NiRuO_{6+\delta}$ is due to the trapping of holes in O_{12} clusters about a $\square_{La}$; the lowest acceptor level must lie above the donor level of the two-electron trap $\square_O^x$, so we place it at an energy above the bottom of the Mn^{4+}/Mn^{3+} couple, Fig. 9(b).

ACKNOWLEDGMENTS

The authors are grateful to the National Science Foundation and the Robert A. Welch Foundation of Houston, TX, for financial support.

[1] A. Wold, R. J. Arnott, and J. B. Goodenough, J. Appl. Phys. **29**, 387 (1958).
[2] J. B. Goodenough, A. Wold, R. J. Arnott, and N. Menyuk, Phys. Rev. **124**, 373 (1961).
[3] G. Blasse, J. Phys. Chem. Solids **26**, 1969 (1965).
[4] J. M. Paulsen, C. L. Thomas, and J. R. Dahn, J. Electrochem. Soc. **147**, 861 (2000).
[5] K. Asai, H. Sekizawa, and S. Iida, J. Phys. Soc. Jpn. **47**, 1054 (1979).
[6] M. Sonobe and K. Asai, J. Phys. Soc. Jpn. **61**, 4193 (1992).
[7] M. C. Sánchez, J. García, J. Blasco, G. Subías, and J. Pérez-Cacho, Phys. Rev. B **65**, 144409 (2002).
[8] J. Blasco, M. C. Sánchez, J. Pérez-Cacho, J. García, G. Subías, and J. Campo, J. Phys. Chem. Solids **63**, 781 (2002).
[9] M. Pechini, U.S. Patent No. 3,330,697 (1967).
[10] V. L. Joseph Joly, P. A. Joy, S. K. Date, and C. S. Gopinath, Phys. Rev. B **65**, 184416 (2002).
[11] R. I. Dass and J. B. Goodenough, Phys. Rev. B **67**, 014401 (2003).
[12] R. I. Dass and J. B. Goodenough, Phys. Rev. B **63**, 064417 (2001).
[13] J. B. Goodenough and R. I. Dass, Int. J. Inorg. Mater. **2**, 3 (2000).
[14] G. A. Novak and A. A. Colville, Am. Mineral. **74**, 488 (1989).
[15] J. A. Ibers, D. H. Templeton, B. K. Vainshtein, G. E. Bacon, and K. Lonsdale, in *International Tables for X-ray Crystallography*, edited by C. H. Macgillavry, G. D. Rieck, and K. Lonsdale (Birmingham, England, 1962), Vol. III, Sec. 3.3, p. 201.
[16] J. A. M. Van Roosmalen, E. H. P. Cordfunke, R. B. Helmholdt, and H. W. Zandbergen, J. Solid State Chem. **110**, 100 (1994).
[17] J. A. M. Van Roosmalen and E. H. P. Cordfunke, J. Solid State Chem. **110**, 106 (1994).
[18] B. C. Tofield and W. R. Scott, J. Solid State Chem. **10**, 183 (1974).
[19] J. F. Mitchell, D. N. Argyriou, C. D. Potter, D. G. Hinks, J. D. Jorgensen, and S. D. Bader, Phys. Rev. B **54**, 6172 (1996).
[20] J. B. Goodenough, J.-S. Zhou, and J. Chen, Phys. Rev. B **47**, 5275 (1993).
[21] R. I. Dass, J.-Q. Yan, and J. B. Goodenough (unpublished).
[22] T. Ohzuku, S. Takeda, and M. Iwanaga, J. Power Sources **81–82**, 90 (1999).
[23] K. R. Poeppelmeier, M. E. Leonowicz, and J. M. Longo, J. Solid State Chem. **44**, 89 (1982).
[24] J. Zaanen, G. A. Sawatzky, and J. W. Allen, Phys. Rev. Lett. **55**, 418 (1985).
[25] J. B. Goodenough and P. M. Raccah, J. Appl. Phys. **36**, 1031 (1965).